NASA
Technical
Paper
2810

1988

Static Mechanical Properties of 30 × 11.5 - 14.5, Type VIII Aircraft Tires of Bias-Ply and Radial-Belted Design

Pamela A. Davis
and Mercedes C. Lopez

Langley Research Center
Hampton, Virginia

National Aeronautics
and Space Administration

Scientific and Technical
Information Division

Contents

Summary

An investigation was conducted to determine the static mechanical characteristics of 30 × 11.5 – 14.5 bias-ply and radial-belted aircraft tires. The tire characteristics were determined by application of vertical and lateral loadings. Mass moment of inertia data were also obtained. The results of the study are presented to show static load deflection curves, spring rates, hysteretic losses, and inertia data. The advantages and disadvantages of each type of tire are also given.

Introduction

Radial-belted tires have been used in the automotive industry for more than 20 years. Despite the benefits of radial-belted automotive tires (i.e., longer tread life, cooler operating temperatures, and improved friction characteristics), the general belief in the aircraft landing-gear industry up until 1980 was that the mechanical properties of these radial-belted tires were unacceptable for aircraft use. For example, landing-gear designers were concerned about lateral forces during crosswind landings (ref. 1) exceeding tire-wheel coupling capability, about tire fore-and-aft stiffness characteristics degrading the performance characteristics of aircraft antiskid braking systems (ref. 2), and about the adverse influence of greatly reduced tire vertical stiffness characteristics on aircraft landing dynamics response.

Continuing research efforts of several tire manufacturers, however, have resulted in radial aircraft tire designs which appear to overcome many of the problems and have been successfully tested on several different aircraft (ref. 1). Thus, the benefits associated with radial-belted automotive tires may also be realized for radial-belted aircraft tires. The emergence of technology for radial-belted aircraft tires has also created a need for a data base of the mechanical properties of radial-belted tires for use in the prediction of landing-gear dynamic response characteristics. The NASA Langley Research Center, in cooperation with the Federal Aviation Administration and the U.S. landing-gear industry, has initiated a research effort to study the mechanical properties and friction characteristics of radial-belted and bias-ply tires under a variety of operating conditions.

The purpose of this paper is to present static loading results from an investigation of the mechanical characteristics of 30 × 11.5 – 14.5 bias-ply and radial-belted aircraft tires. Static characteristics were obtained over a range of inflation pressures from 245 to 310 psi, vertical loads up to 25 000 lb, and lateral loads up to 4000 lb. The parameters measured included tire stiffness characteristics, damping, and inertia properties. A comparison of the mechanical properties for the two tire designs is also presented.

The tires and wheel assemblies were supplied by the U.S. Air Force, although the bias-ply and radial-belted tires were from two different manufacturers. Prior to static loading tests at Langley, each tire was preconditioned at the Wright Aeronautical Laboratories, Vehicle Equipment Division, with 2 miles of taxi tests at 30 mph at rated load and inflation pressure.

Construction of Bias-Ply and Radial-Belted Design

Construction details for the bias-ply and radial-belted 30 × 11.5 – 14.5 tires are shown in figure 1. The bias-ply tire is constructed of numerous laminates of rubber-textile plies that alternate at various angles from 60° near the tire bead to 30° near the crown area of the tire. Multiple bead wires on each side of the tire hold together the large number of plies and form a torus-like shell. The bias-ply tire has a 24-ply rating, and additional plies are laid at some specified angle between the tire carcass and the tread to provide tread reinforcement. The highly stiffened shell and weight of the tire are a result of the ply assembly and multiple-ply casing (ref. 1).

The radial-belted tire uses fewer plies of higher denier textile cords than the bias-ply tire, which results in a weight and volume reduction. The radial-belted tire has casing plies approximately oriented in the plane of the tire cross section, and its size and load-carrying requirements determine the number of plies in the tire. Generally, only one steel-bead wire is needed on each side of the tire, as opposed to multiple bead wires in the bias-ply tire. For the radial-belted tires used in this investigation, a textile cord belt surrounds the casing of the tire circumferentially, and a steel belt surrounds the cord belt and acts as a protector ply. The radial-belted tire has a 26-ply rating (ref. 1). Characteristics of the two types of tires are given in table 1, and the tires are shown in figure 2.

Apparatus and Test Procedure

The bias-ply tire was tested at an inflation pressure of 245 psi and the radial-belted tire was tested at an inflation pressure of 310 psi. The inflation pressures correspond to a 35-percent tire deflection at the rated load of 25 000 lb. The radial tire was also tested at an inflation pressure of 245 psi, which corresponds to a 51-percent tire deflection at the rated load of 25 000 lb. Hence, experimental data were obtained for the bias-ply and radial-belted tires at the same tire deflection and the same inflation pressure.

The test fixture used to measure the mechanical properties of the test tires under static conditions is shown in figure 3. The tire-wheel-axle assembly was mounted on a dynamometer that was instrumented with five strain-gauge beams. Two of the beams were used to measure the vertical load, one beam was used to measure the lateral load, and two beams were used to measure the drag load. The test fixture has one hydraulic cylinder, which applied vertical load to the dynamometer and loaded the tire onto a frictionless table. Another hydraulic cylinder, which was mounted in series with the table, applied lateral load to the tire. The table was instrumented with three load cells mounted to measure the vertical load (fig. 3) and one load cell mounted to measure the lateral load (fig. 4). Displacement transducers were mounted parallel to each hydraulic cylinder to measure tire vertical and lateral displacements. Output data from the various instruments were recorded by a computer (fig. 5) in 1000-lb intervals for the vertical-load tests and in 375-lb intervals for the lateral-load tests. Subsequent to the tests, the data were converted into engineering units and saved for further analysis and evaluation. Figure 6 is a block diagram of the instrumentation layout used to obtain data.

Static pure vertical-loading tests were conducted to measure tire vertical spring rate and energy loss associated with hysteresis using test procedures reported in reference 3. In these tests, load was applied hydraulically until the maximum-rated load of 25 000 lb was reached; the load was then gradually reduced to zero. Vertical load and deflection were continuously monitored during the loading-unloading cycle to produce a load-deflection curve or hysteresis loop. Such data provided an indication of tire vertical-loading behavior and defined the vertical spring rate and the hysteretic loss (ref. 3). For these tests, measurements were taken at four different peripheral positions around each tire.

Lateral-loading tests were conducted to measure tire lateral spring rate and energy loss due to hysteresis (ref. 3). Vertical load was applied and maintained at the tire-rated load of 25 000 lb. Lateral load was gradually applied up to a load of 4000 lb, then reduced to zero; the same loading procedure was then repeated in the opposite direction. Lateral load was limited by tire slippage to the 4000-lb value for the bias-ply tire and 3000 lb for the radial-belted tire. A load-deflection curve was obtained from these results, which define the tire lateral-loading characteristics, lateral spring rate, and hysteretic loss. Lateral tire deflection was measured perpendicular to the wheel plane. This deflection was assumed to be equivalent to the displacement of the frictionless table and was measured by a displacement transducer (fig. 4). The static lateral-loading tests were also conducted at four different peripheral positions around each tire.

Mass moment of inertia of the tires was measured using a torsional pendulum (ref. 4), shown in figure 7. The torsional pendulum used for these tests consisted of two 24-in.-diameter plates bolted together and suspended in parallel by three equally tensioned, 17-ft wire cables attached to an overhead support.

The tare moment of inertia of the two plates was initially determined. Similar tests were conducted with the inflated tire, with the wheel assembly, and with the rotors suspended between the plates. Weight of the plates and tire-wheel assembly were recorded. References 5 and 6 contain a detailed description of the use of torsional pendulums for determination of moment of inertia.

Error Analysis

The results and discussion of random-error calculations are presented in this section. Spring constants were obtained by measuring the slope at specific points of load application and load relief between the extremes of the hysteresis loop. Slopes at the upper limit of the curve were not considered because of the uncertain value of the turnaround point as a result of the mechanical-system limitations. In an effort to quantify the error on slope measurement, the average slope and average deviation of the slopes were computed at each specific point for four peripheral positions on the tire. The ratio of the average deviation to the average slope was then considered to represent the percentage of error (ref. 6). Vertical and lateral spring-rate data for the bias-ply tire were 4.49 percent and 6.4 percent in error, respectively. Vertical spring-rate data for the radial-belted tire were 3.20 percent in error at an inflation pressure of 245 psi and 2.15 percent in error at an inflation pressure of 310 psi. Lateral spring-rate values for the radial-belted tire at inflation pressures of 245 and 310 psi were 3.70 percent and 5.0 percent in error, respectively. The area of each load-deflection loop was measured three times. Average area and average deviation of the area were then computed to obtain the percentage error. Vertical load-deflection loops had a 1.03-percent error for the bias-ply tire and 1.65-percent and 2.59-percent errors for the radial-belted tire at inflation pressures of 245 and 310 psi, respectively. For the lateral load-deflection loops, percentages of error were found to be 0.94 percent for the bias-ply tire and 2.66 percent and 3.44 percent for the radial-belted tire at inflation pressures of 245 and 310 psi.

Accuracy of the experimental data points has been computed based on calibration and instrumentation accuracy. Reading errors from all nine channels of data were computed; the voltage readings plus or minus the manufacturer's instrumentation accuracy factors were taken as theoretical values, and the voltage readings themselves were taken as experimental values. Experimental values were subtracted from the theoretical values and divided by the theoretical values to obtain the percentage of error. Maximum and minimum voltage responses from each channel were considered and analyzed. Large error percentages were expected for low voltage response because of the voltage ranges available for each sensor. Calibration errors were obtained from linear curve fittings that were obtained by calibrating the load cells in the test setup. Calibration and instrumentation percentage errors were then added to the reading errors to obtain the total error percentage.

Standard vertical-load data from the load cells were 0.61 percent in error for both minimum and maximum voltage. Lateral standard-load data were 0.66 percent and 0.61 percent in error for minimum and maximum voltage, respectively. Vertical and lateral displacement readings both indicated a 0.6 percent error for both voltage conditions.

To compute the error for the polar moment of inertia values, the error for each term of equation (2) was found individually by using the same method described previously for the slope, for the area, and then for a combination of both. Each individual percentage of error was multiplied by the power it was raised to in the equation and then squared to obtain its square contribution. The square root of the sum of the square contributions was then considered as the total error. Polar moment of inertia was found to be 3.10 percent in error for the bias-ply tire and 3.12 percent in error for the radial-belted tire. The major source of error of the individual terms in these calculations was the measurement of the radius of the plates; there was an average deviation of 0.06 in.

Results and Discussion

Static Vertical Loading

Static vertical-loading tests were made for two $30 \times 11.5 - 14.5$ bias-ply and radial-belted tires. Results of these tests are presented to show vertical-load-deflection curves, vertical spring rate, and hysteretic losses. Table 2 gives static vertical-load data in engineering units.

Load deflection. Four load-deflection curves were generated for each tire. A typical load-deflection curve for the bias-ply tire is shown in figure 8, where the lower bound of tire vertical stiffness is represented by the load-application curve, and the upperbound of tire vertical stiffness is represented by initial load relief (ref. 3). The data in figure 8 show that the vertical deflection is nonlinear at the initial load application up to 6000 lb (0.75-in. deflection) and at the maximum load-deflection point of 25 000 lb (2.4-in. deflection) but linear over the majority of the load-application range. Analagous load-deflection characteristics apply to the load-relief range. Also, the loading and unloading process shows some hysteresis as a result of energy loss during this process. Similar load-deflection curves were obtained for the radial-belted tire at inflation pressures of 310 and 245 psi. (See figs. 9 and 10.) Data in the figures indicate that the load deflection is nonlinear during the entire load-application and load-relief cycles.

Spring rate. Vertical spring rate was obtained by measuring the instantaneous slope at various points along the vertical load-deflection curves. Vertical spring rate for the bias-ply tire is plotted as a function of vertical deflection in figure 11. A regression-analysis technique was used to fit a curve through the spring-rate data. At initial load application, the spring rate increases linearly from 7500 lb/in. to 11 500 lb/in. and remains constant at this maximum value for the remainder of the load application. A maximum spring constant of 15 000 lb/in. is observed at initial load relief and is nonlinear as it decreases to 11 500 lb/in.

Vertical spring rates for the radial-belted tire at inflation pressures of 310 and 245 psi are shown as a function of vertical deflection in figures 12 and 13, respectively. For both inflation pressures, the tire spring rate is nonlinear during the load application and initial load relief. The maximum spring rates for the radial-belted tire were 14 500 lb/in. and 11 500 lb/in. at 310 psi inflation pressure and 245 psi inflation pressure, respectively.

Data in figures 11 and 12 indicate that the vertical stiffness characteristics of the bias-ply tire at an inflation pressure of 245 psi and the radial-belted tire at an inflation pressure of 310 psi are very similar. One implication of the similarity of these results is that the landing dynamic characteristics of an aircraft equipped with this radial-belted tire would be similar to those of one equipped with a standard bias-ply tire. Data in figures 11 and 13 indicate that, as a result of the lower inflation pressure of 245 psi, the radial-belted tire is less stiff than the bias-ply tire.

Hysteretic loss. Hysteretic loss is represented by the enclosed area of the curves presented in

figures 8 through 10. As can be seen, the hysteresis is less for the radial-belted tire at an inflation pressure of 310 psi than for the bias-ply tire. This distinction suggests that there is less heat generated in the radial-belted tire during the loading and unloading cycle. The hysteresis for the radial-belted tire at 245 psi inflation pressure is greater than for the bias-ply tire at the same inflation pressure (figs. 8 and 10) because of the radial-belted tire deflection of 51 percent versus the bias-ply tire deflection of 35 percent. The average vertical hysteresis is 2819 in-lb for the bias-ply tire, 2547 in-lb for the radial-belted tire with an inflation pressure of 310 psi, and 2945 in-lb for the radial-belted tire with an inflation pressure of 245 psi.

Static Lateral Loading

Static lateral-loading tests were made for 30 × 11.5 – 14.5 bias-ply and radial-belted tires. Results of these tests are presented to show load-deflection curves, lateral spring rate, and hysteretic loss of the tires. Static lateral-load data are presented in table 2.

Load deflection. A typical lateral-load-deflection curve for the bias-ply tire is shown in figure 14. After the rated load of 25 000 lb was applied vertically, the tire was loaded laterally, beginning at zero lateral load. Data in figure 14 show that the lateral deflection is linear at the initial load-application range up to approximately 0.2 in. The remainder of the load-application curve is linear, but at a less-steep slope. This less-steep slope indicates a much stiffer spring at initial load application. Similar load-deflection characteristics apply to the load-relief range and to the loading and unloading cycle in the opposite direction.

Figures 15 and 16 are plots of the lateral-load-deflection curve of the radial-belted tire at inflation pressures of 310 and 245 psi, respectively. The load was applied in a similar manner as for the bias-ply tire, and similar spring stiffness relationships were observed for the radial-belted tire at each inflation pressure. However, the maximum lateral load was ±3000 lb because of tire slippage on the frictionless table that prevented testing to higher loads.

Spring rate. The lateral spring rates for each tire are determined from the instantaneous slope of the lateral-load-deflection curves. In figure 17, the lateral spring rate for the bias-ply tire is plotted as a function of lateral deflection, and a regression analysis is used to fit a curve through these points. The spring rate is linear during the load-application cycle and nonlinear at initial load relief, where the maximum spring rate of 8000 lb/in occurs.

The lateral spring rate for the radial-belted tire is shown in figures 18 and 19. As with the bias-ply tire, the slope of the lateral-load-deflection curve for the radial-belted tire at an inflation pressure of 310 psi is nearly linear during load application, which results in a nearly constant spring rate of 4250 lb/in. The maximum spring rate of 5300 lb/in. is obtained at initial load relief. The radial-belted tire at an inflation pressure of 245 psi has characteristics similar to the radial-belted tire at the rated inflation pressure of 310 psi. At initial load relief there is a maximum spring rate of 5000 lb/in. A comparison of the three spring-rate plots indicates that the lateral stiffness of the radial-belted tire with an inflation pressure of 310 psi is nearly equivalent to that of the bias-ply tire with an inflation pressure of 245 psi. If the radial-belted tire is operated at 245 psi, its lateral-stiffness values are 13 to 20 percent less than for the bias-ply tire at the same inflation pressure.

Hysteretic loss. Since the maximum lateral load was 1000 lb less for the radial-belted tire than for the bias-ply tire because of slippage problems between the radial-belted tire tread and the frictionless table, a comparison between the bias-ply tire and radial-belted tire could not be made. The hysteretic loss for the bias-ply tire is 1605 in-lb; the hysteretic loss for the radial-belted tire is 749 in-lb at an inflation pressure of 310 psi and 758 in-lb at an inflation pressure of 245 psi. The radial-belted tire expended more energy at the lower inflation pressure than at its rated inflation pressure.

Mass Moment of Inertia

The mass moment of inertia for each tire design and the tare inertia for the two pendulum plates (fig. 7) were calculated using the following equation:

$$J_{\text{plates}} = \frac{\tau^2 W R^2}{4\pi^2 L} \tag{1}$$

where

J mass moment of inertia, in-lb-sec^2

τ average period of system oscillation, sec

W weight of object being measured, lb

R radial distance from center of plate to support cables, in.

L length of support cables, in.

The mass moment of inertia of the tire and rotating parts is calculated using the following equation:

$$J_{\text{tire}} = \frac{\tau^2 W R^2}{4\pi^2 L} - J_{\text{plates}} \tag{2}$$

where

$$J_{\text{plates}} = 4.35 \text{ in-lb-sec}^2$$

The respective moment of inertia values were 31.51 in-lb-sec^2 for the bias-ply tire and 27.74 in-lb-sec^2 for the radial-belted tire. Thus, the moment of inertia of the radial-belted tire is 12 percent less than that of the bias-ply tire, which suggests that the radial-belted tire would require slightly less energy to spin up during the landing touchdown than the bias-ply tire. Less energy in spin-up could mean reduced tread wear for the radial-belted tire during high-speed landings.

Conclusions

An investigation has been conducted to determine and compare the static mechanical characteristics of 30 × 11.5 – 14.5 bias-ply and radial-belted aircraft tires. Stiffness and damping characteristics were obtained from load-deflection curves under various static loading conditions. Inertia properties of the test articles were obtained using a torsional pendulum. The results of this investigation indicate the following conclusions:

1. Vertical stiffness characteristics obtained for the radial-belted tire and the bias-ply tire at inflation pressures of 310 psi and 245 psi, respectively, were similar. The radial-belted tire at an inflation pressure of 245 psi showed less vertical stiffness than the bias-ply tire at the same inflation pressure.
2. Lateral stiffness of the radial-belted tire with an inflation pressure of 310 psi was comparable to that of the bias-ply tire with an inflation pressure of 245 psi. At 245 psi inflation pressure, the lateral stiffness of the radial-belted tire was less than the lateral stiffness of the bias-ply tire.
3. Hysteretic loss of the radial-belted tire at an inflation pressure of 310 psi is significantly less than the hysteretic loss of the bias-ply tire at an inflation pressure of 245 psi under vertical loading conditions. This result indicates the radial-belted tire generates less heat during normal operation and, therefore, runs cooler.
4. The radial-belted tire requires less energy to spin up than the bias-ply tire under the same touchdown conditions. Consequently, there could be a reduction in tread wear for the radial-belted tire during high-speed landings.

NASA Langley Research Center
Hampton, VA 23665-5225
March 22, 1988

References

1. Cesar, J. P.; Musy, J.; and Olds, R.: Development of Radial Aircraft Tires. Michelin paper presented to 38th International Air Safety Seminar (Boston, Massachusetts), Nov. 4–7, 1985.
2. Tanner, John A.: *Fore-and-Aft Elastic Response Characteristics of 34 × 9.9, Type VII, 14 Ply-Rating Aircraft Tires of Bias-Ply, Bias-Belted, and Radial-Belted Design.* NASA TN D-7449, 1974.
3. Tanner, John A.; Stubbs, Sandy M.; and McCarty, John L.: *Static and Yawed-Rolling Mechanical Properties of Two Type VIII Aircraft Tires.* NASA TP-1863, 1981.
4. Tanner, John A.; Stubbs, Sandy M.; Dreher, Robert C.; and Smith, Eunice G.: *Dynamics of Aircraft Antiskid Braking Systems.* NASA TP-1959, 1982.
5. Volterra, Enrico; and Zachmanoglou, E. C.: *Dynamics of Vibrations.* Charles E. Merrill Books, Inc., c.1965, pp. 58–60.
6. Beers, Yardley: *Introduction to the Theory of Error, Second ed.* Addison-Wesley Publ. Co., 1962.

Table 1. Characteristics of Bias-Ply and Radial-Belted Tires

Parameter	Bias-ply	Radial-belted
Size	30 × 11.5 – 14.5	30 × 11.5 – 14.5
Ply rating	24	26
Weight, lb	68.75	55.5
Rated vertical load, lb	25 000	25 000
Rated inflation pressure at 35 percent load deflection, psi	245	310
Outside diameter of unloaded tire, in.	30	30
Maximum carcass width of unloaded tire, in.	8	8
Tread grooves	3	4

Table 2. Static-Load Test Data

(a) Vertical loading

Bias-ply at 245 psi		Radial-belted at 310 psi		Radial-belted at 245 psi	
Load, lb	Deflection, in.	Load, lb	Deflection, in.	Load, lb	Deflection, in.
0.000	0.000	0.000	0.000	0.000	0.000
703.666	.146	725.007	.150	752.869	.178
1704.330	.290	1706.109	.297	1757.683	.347
2705.587	.422	2710.922	.429	2753.605	.495
3703.880	.544	3709.215	.549	3751.305	.636
4705.137	.660	4722.328	.665	4754.340	.771
5704.023	.762	5720.029	.775	5752.633	.903
6704.094	.862	6711.800	.885	6778.788	1.034
7704.758	.958	7711.279	.991	7769.374	1.154
8704.237	1.049	8707.201	1.095	8758.182	1.274
9705.494	1.142	9709.050	1.196	9758.254	1.391
10704.379	1.233	10719.792	1.297	10757.139	1.510
11705.043	1.324	11722.235	1.392	11755.432	1.621
12706.893	1.412	12719.342	1.486	12753.132	1.732
13704.000	1.494	13714.078	1.577	13752.611	1.840
14704.072	1.580	14710.593	1.668	14744.976	1.948
15704.736	1.669	15712.442	1.759	15747.418	2.054
16704.214	1.758	16714.885	1.848	16746.897	2.158
17704.286	1.845	17709.621	1.935	17746.968	2.260
18704.357	1.935	18710.878	2.023	18753.560	2.359
19704.428	2.026	19708.578	2.109	19751.853	2.454
20709.242	2.111	20702.128	2.194	20747.775	2.551
21705.164	2.196	21707.535	2.278	21747.846	2.647
22704.642	2.287	22705.828	2.361	22749.696	2.745
23704.121	2.378	23708.270	2.441	23747.989	2.840
24704.192	2.468	24708.934	2.520	24930.053	2.954
24286.261	2.437	24161.770	2.495	24196.746	2.905
23291.525	2.384	23167.034	2.431	23190.747	2.829
22295.010	2.318	22154.514	2.362	22193.639	2.747
21295.532	2.244	21158.592	2.290	21190.604	2.658
20293.687	2.168	20168.599	2.217	20195.275	2.569
19295.389	2.087	19153.707	2.140	19199.354	2.477
18295.318	2.008	18150.672	2.060	18195.725	2.384
17295.246	1.928	17135.780	1.979	17200.397	2.289
16292.211	1.845	16128.595	1.897	16200.325	2.190
15295.697	1.761	15136.230	1.814	15197.290	2.090
14293.254	1.676	14135.566	1.729	14184.177	1.987
13295.554	1.592	13133.717	1.641	13185.884	1.885
12294.297	1.507	12140.759	1.552	12186.405	1.778
11293.633	1.419	11142.466	1.460	11192.262	1.668
10295.933	1.333	10140.616	1.365	10196.933	1.556
9295.269	1.243	9143.509	1.267	9200.419	1.440
8295.790	1.149	8148.180	1.167	8199.755	1.322
7293.940	1.050	7149.887	1.064	7204.426	1.198
6295.055	.953	6146.259	.957	6172.936	1.069
5293.798	.848	5145.595	.848	4973.087	.935
4296.098	.739	4150.859	.733	4086.243	.814
3296.028	.620	3136.560	.609	3186.356	.680
2293.584	.485	2142.417	.483	2153.088	.525
1295.291	.343	1148.274	.338	1158.945	.363
1295.291	.326	154.131	.162	184.364	.153

Table 2. Continued

(b) Lateral loading

Bias-ply at 245 psi		Radial-belted at 310 psi		Radial-belted at 245 psi	
Load, lb	Deflection, in.	Load, lb	Deflection, in.	Load, lb	Deflection, in.
−3.614	0.000	0.000	0.000	0.000	0.000
472.614	−.073	12.448	.049	15.259	.026
1071.715	.073	329.666	.124	330.469	.107
1670.413	.223	706.312	.209	704.706	.204
2267.907	.379	1087.776	.297	1079.745	.306
2866.605	.535	1462.013	.390	1452.778	.411
3463.296	.690	1834.644	.489	1829.424	.527
4061.995	.844	2212.494	.586	2202.456	.639
3703.820	.810	2584.723	.677	2576.692	.753
3106.326	.706	2992.288	.791	2984.659	.884
2504.013	.593	2655.796	.743	2651.379	.825
1903.709	.468	2281.559	.671	2275.536	.744
1305.412	.340	1904.913	.592	1898.489	.655
708.721	.204	1531.480	.513	1527.063	.565
113.235	.059	1158.046	.428	1152.424	.463
−482.653	−.097	783.809	.342	769.354	.366
−1081.753	−.252	393.109	.261	395.920	.267
−1681.656	−.412	31.320	.172	24.896	.169
−2280.756	−.571	−342.917	.107	−353.357	−.061
−2878.250	−.728	−717.153	.003	−725.987	−.039
−3476.146	−.943	−1092.595	−.103	−1101.830	−.147
−4072.033	−1.091	−1466.028	−.196	−1476.067	−.255
−3714.661	−1.046	−1842.273	−.288	−1851.107	−.362
−3117.167	−.946	−2218.919	−.382	−2226.548	−.472
−2517.666	−.840	−2594.360	−.477	−2599.580	−.584
−1921.778	−.719	−2960.165	−.592	−3004.334	−.718
−1319.064	−.599	−2662.221	−.541	−2671.055	−.665
−721.570	−.468	−2289.189	−.471	−2291.999	−.584
−123.675	−.334	−1916.558	−.397	−1917.763	−.501
		−1535.897	−.318	−1545.132	−.413
		−1162.864	−.243	−1168.085	−.320
		−784.612	−.160	−793.446	−.222
		−414.792	−.078	−420.013	−.123
		−44.973	−.008	−44.973	−.024

Table 2. Continued

(c) Vertical spring rate

Deflection, in.	Spring rate, lb/in.			
	Position 1	Position 2	Position 3	Position 4
Bias-ply at 245 psi				
0.30	7812	7083	6704	7273
.40	8125	8000	8627	8000
.50	8718	8649	9118	8667
.60	10000	9545	9523	9022
.80	10769	11500	10345	10638
.90	11111	11111	11039	10869
1.00	11429	11702	11429	11351
1.30	11842	11607	11475	11403
1.50	11719	11667	11354	11546
2.40	11719	11667	11354	11546
2.30	15000	15000	14286	14444
2.20	14286	14667	13857	14200
2.00	12667	13529	12872	13000
1.80	11868	12200	11937	12154
1.40	12000	11719	11429	11702
1.20	11488	11173	11076	11329
Radial-belted at 310 psi				
0.30	7285	7027	7133	7226
.40	7750	7698	7867	7962
.50	8276	8153	8333	8182
.60	8713	8456	8652	8477
.90	9714	9580	9375	9512
1.50	11161	10648	10598	11017
2.40	12708	12101	12182	12300
2.30	14500	13889	14167	13889
2.20	13736	13596	13021	13235
1.90	12072	11875	11905	11927
1.50	11101	10873	10882	10940
1.30	10417	10417	10000	10769
Radial-belted at 245 psi				
0.30	5878	6299	5769	5732
.40	6296	6554	6149	6457
.50	6687	6857	6443	6643
.60	6943	7063	6867	7055
.90	7785	7609	7744	7467
1.50	8873	8561	8931	8462
2.40	10000	10089	9504	9677
2.90	10973	10855	10317	10522
2.70	11525	11204	11748	11333
2.50	10769	10741	10727	10943
2.20	10000	10248	9846	9737
1.90	9394	9487	9224	9219
1.50	8797	8492	8443	8504

Table 2. Concluded

(d) Lateral spring rate

Deflection, in.	Spring rate, lb/in.			
	Position 1	Position 2	Position 3	Position 4
Bias-ply at 245 psi				
0.20	3744	3951	3846	4000
.40	3729	3884	3814	3917
.60	3797	3851	3835	3906
.80	3737	3831	3838	3900
.85	(a)	7692	8333	(a)
.80	(a)	6765	5882	6667
.70	4902	5833	5109	5556
.65	4600	5556	4833	5172
.58	4348	5147	4677	4808
.46	4348	4730	4800	4545
.34	4286	4412	4545	4412
Radial-belted at 310 psi				
0.20	4360	4323	4257	4069
.40	4122	4150	4013	3961
.66	(a)	(a)	5526	5000
.60	4687	5000	5000	4762
.52	4687	(a)	(a)	(a)
.54	(a)	5000	4808	4687
.43	4250	(a)	(a)	(a)
.44	(a)	4545	4545	4412
.34	4167	(a)	(a)	4375
.38	(a)	4545	4444	(a)
.30	(a)	4333	4286	(a)
Radial-belted at 245 psi				
0.20	3606	3576	3594	3654
.40	3433	3462	3469	3480
.60	3399	3333	3364	3229
.80	3238	3148	3235	3179
.82	4827	4896	5000	4815
.70	4057	4423	4085	4345
.50	3846	3889	3859	3989
.78	4808	4545	4545	4500
.62	4167	4167	4286	4000
.40	3750	3846	3864	3788

[a]Data not available at this deflection.

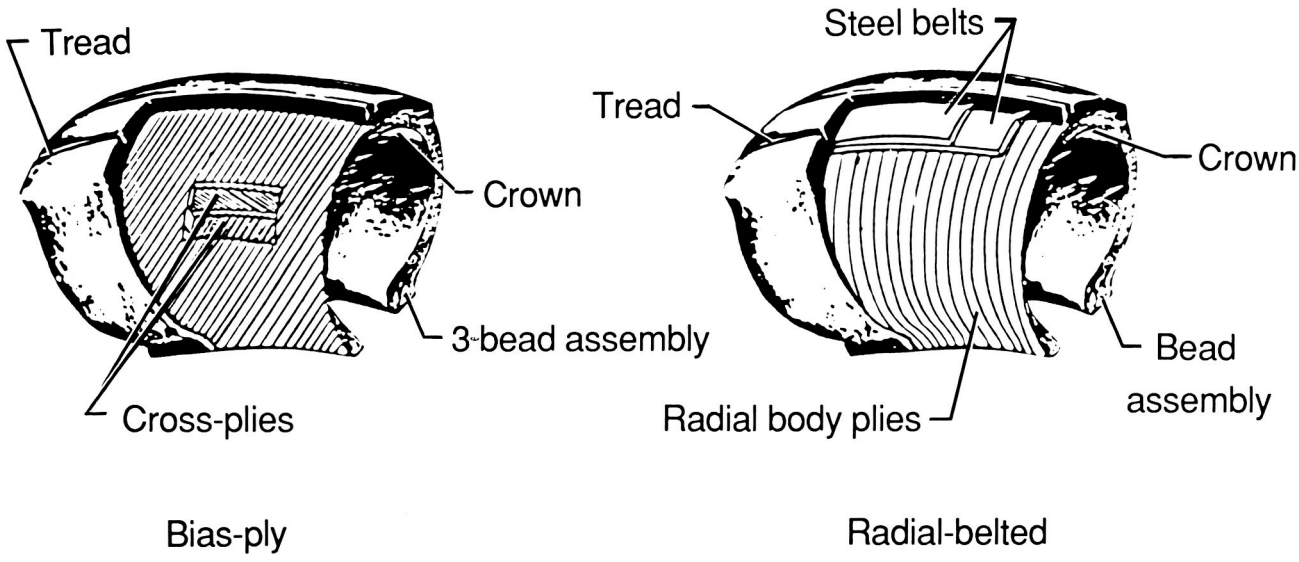

Figure 1. Bias-ply and radial-belted tire construction.

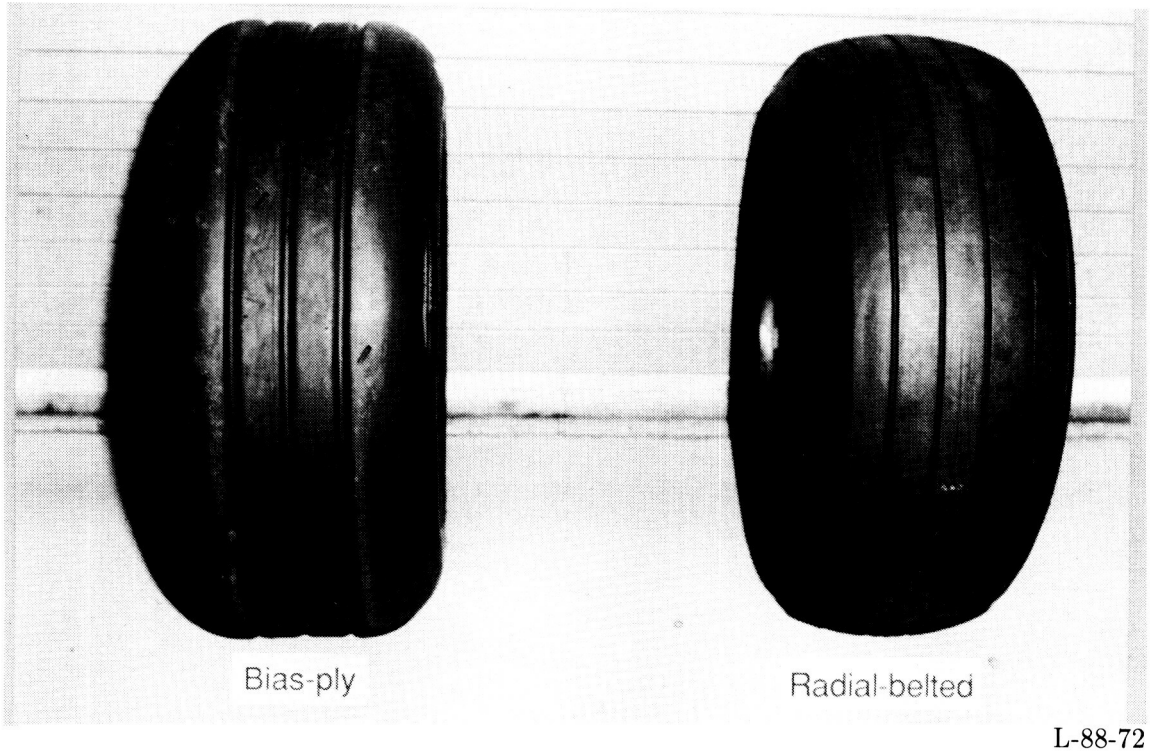

Figure 2. Uninflated bias-ply and radial-belted 30 × 11.5 – 14.5 test tires.

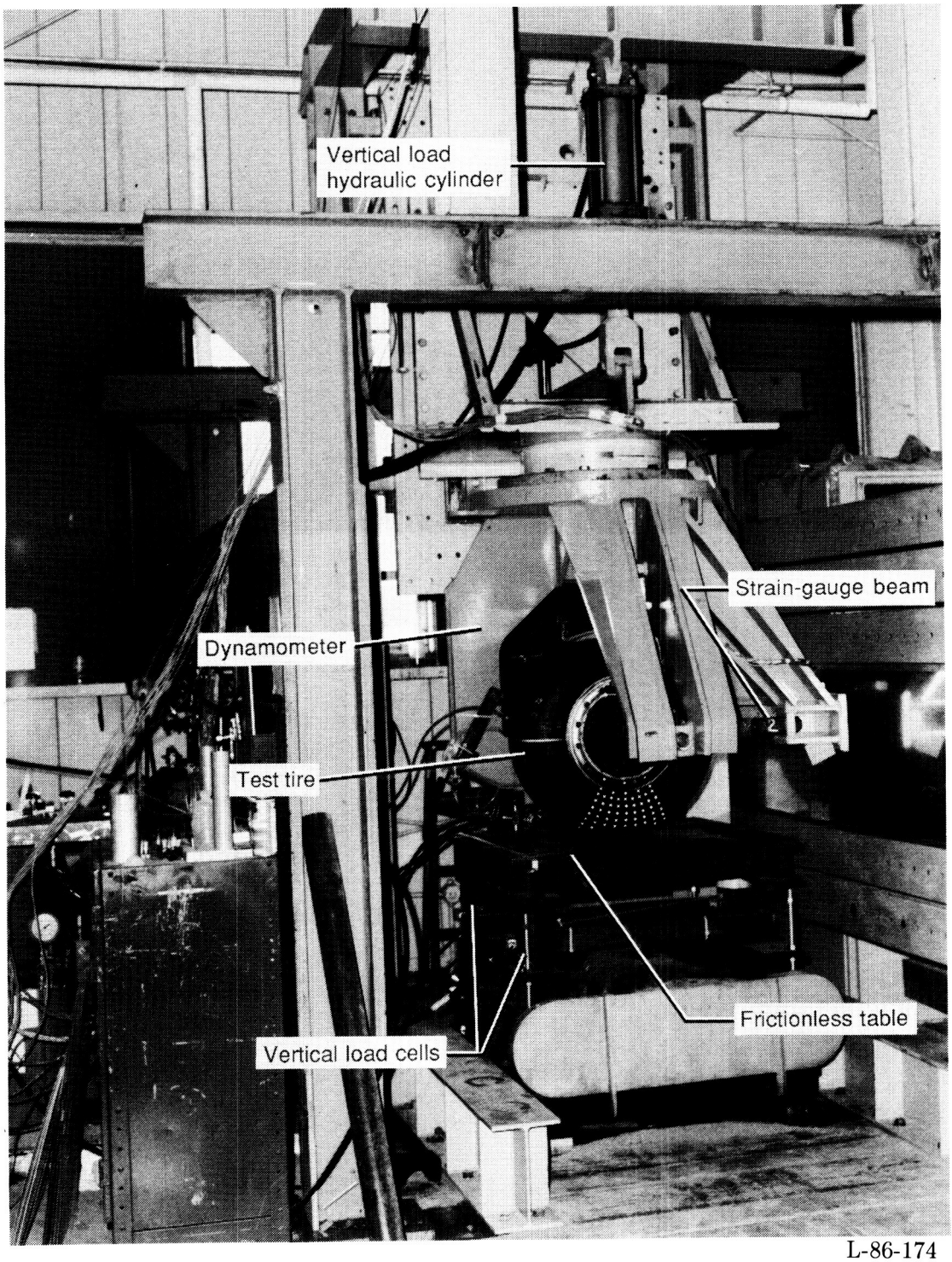

L-86-174

Figure 3. Static test fixture.

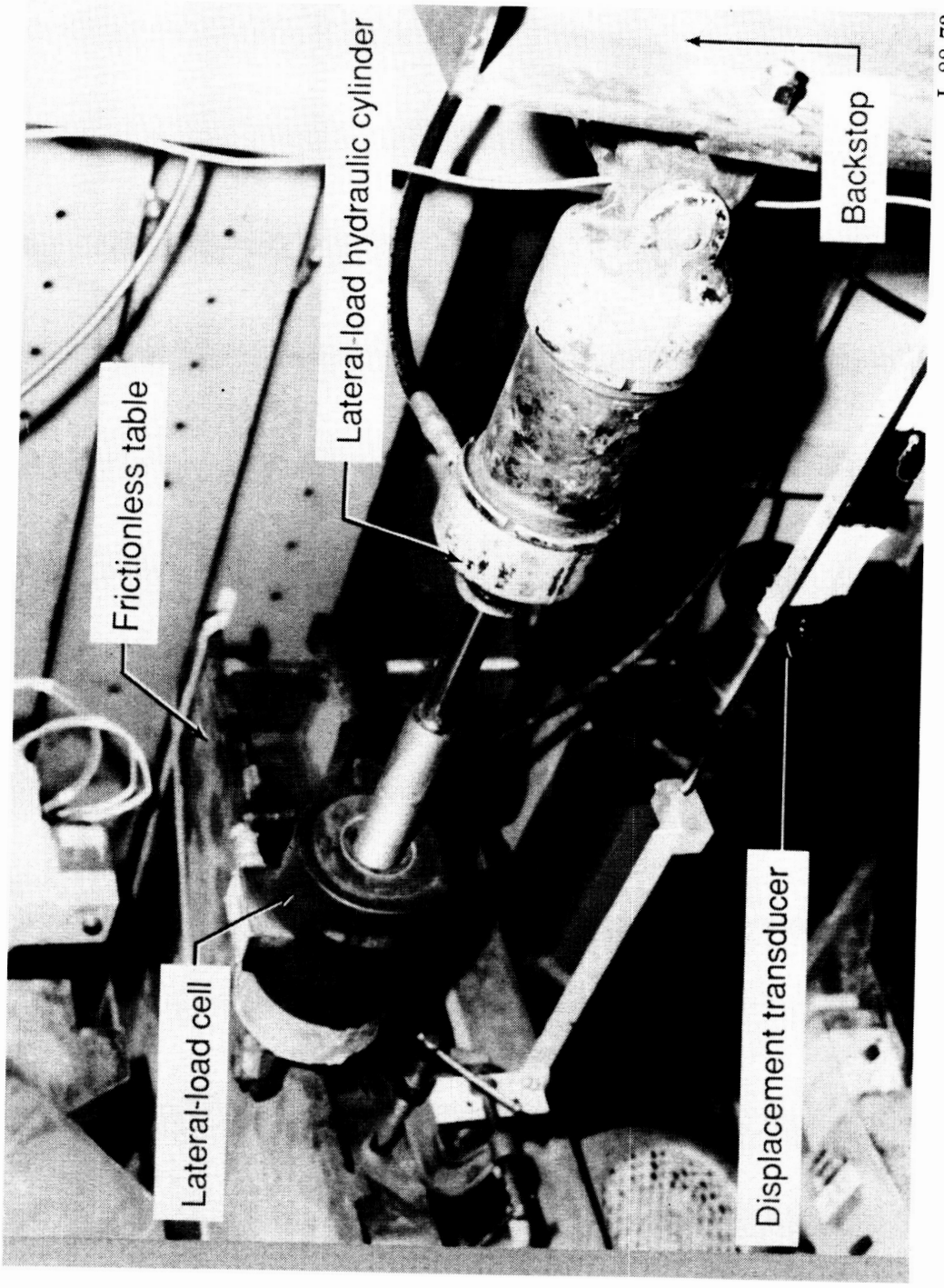

Figure 4. Lateral-load measurement setup (rear view of fig. 3).

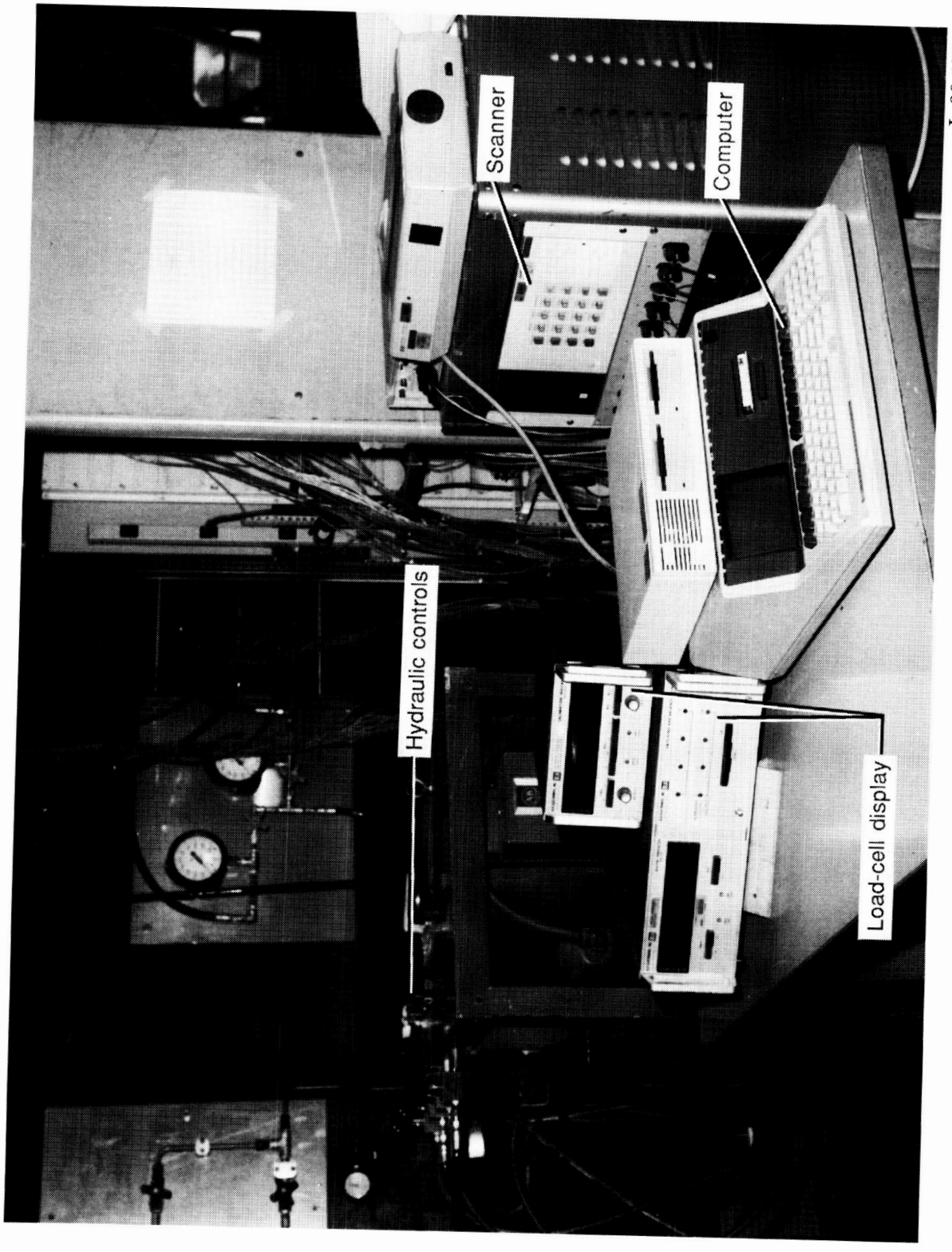

L-86-178

Figure 5. Instrumentation setup for static loading tests.

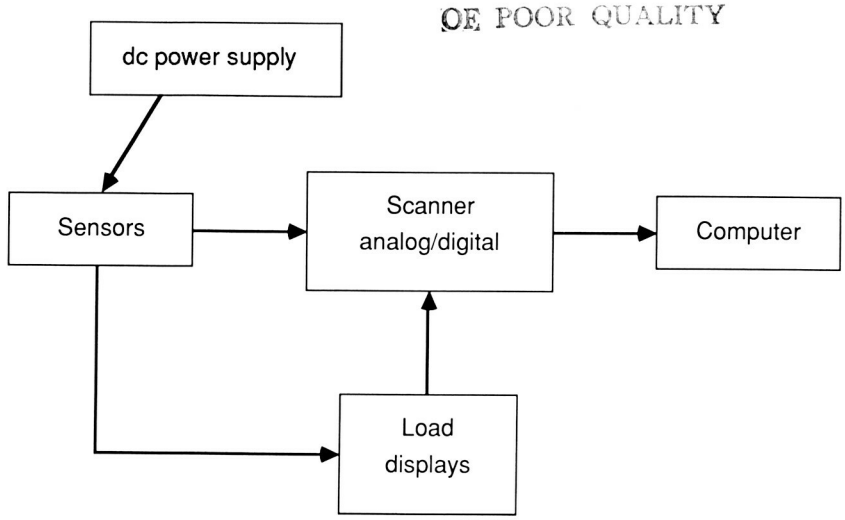

Figure 6. Instrumentation logic.

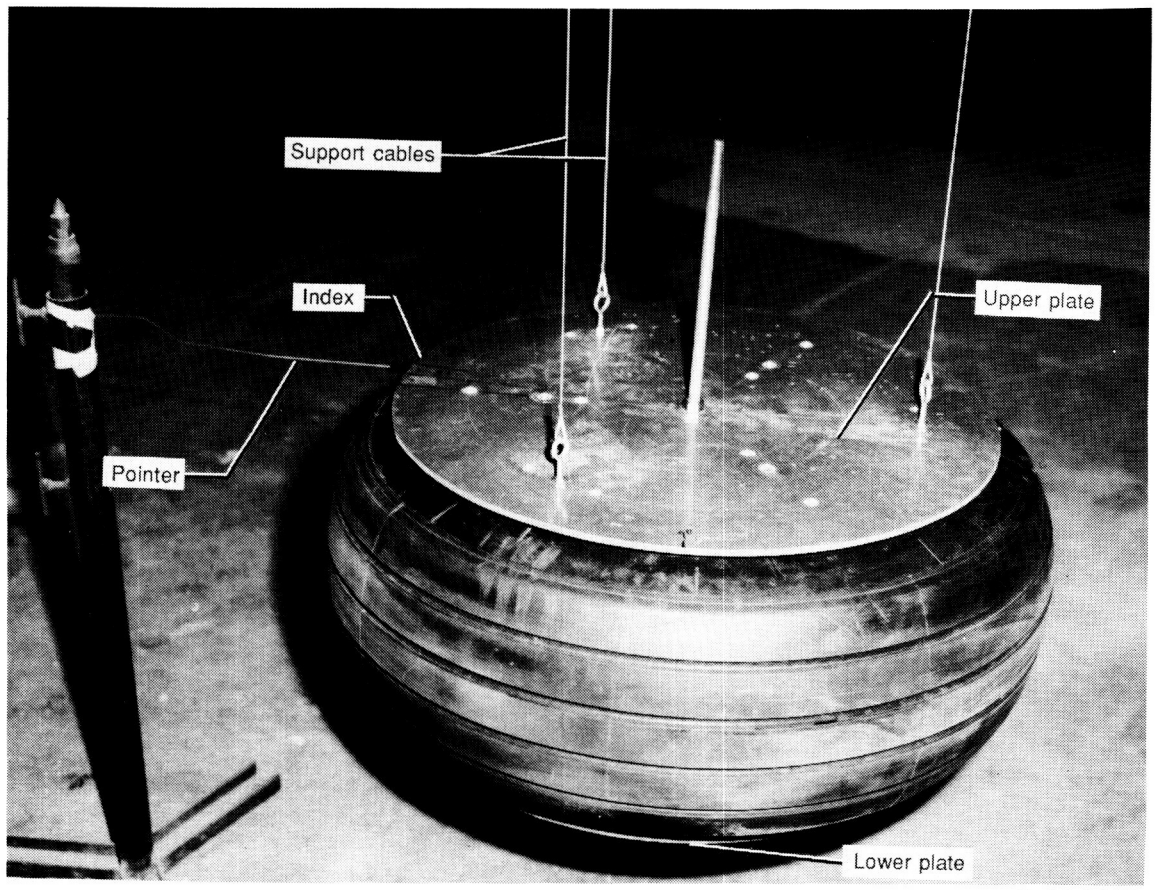

L-86-1586

Figure 7. Torsional pendulum test fixture.

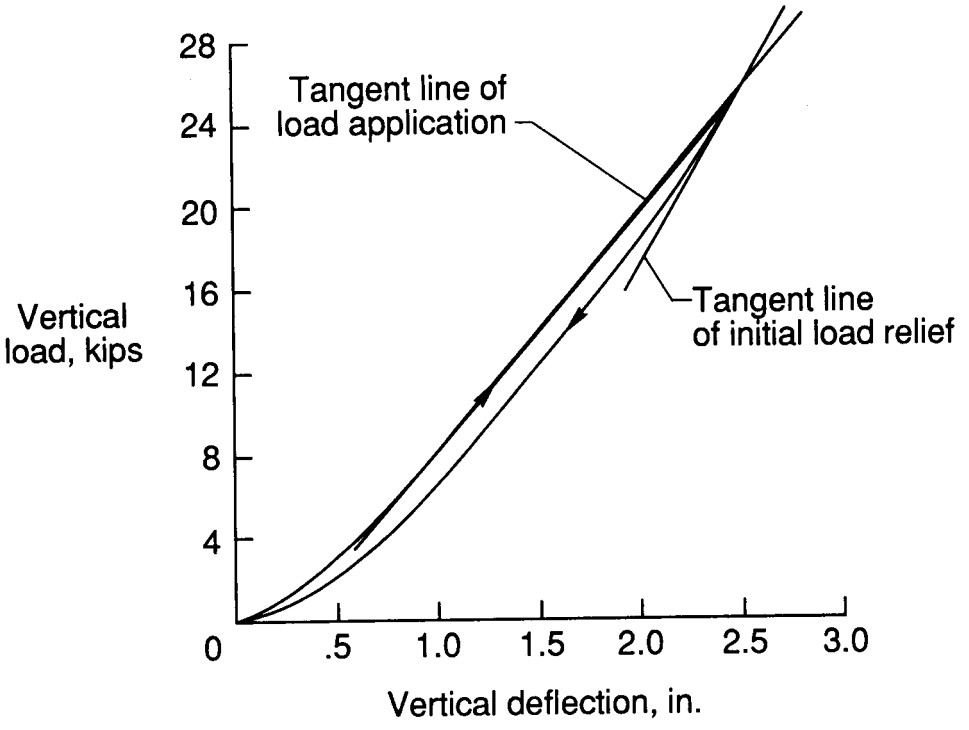

Figure 8. Vertical-load-deflection curve of bias-ply tire at inflation pressure of 245 psi.

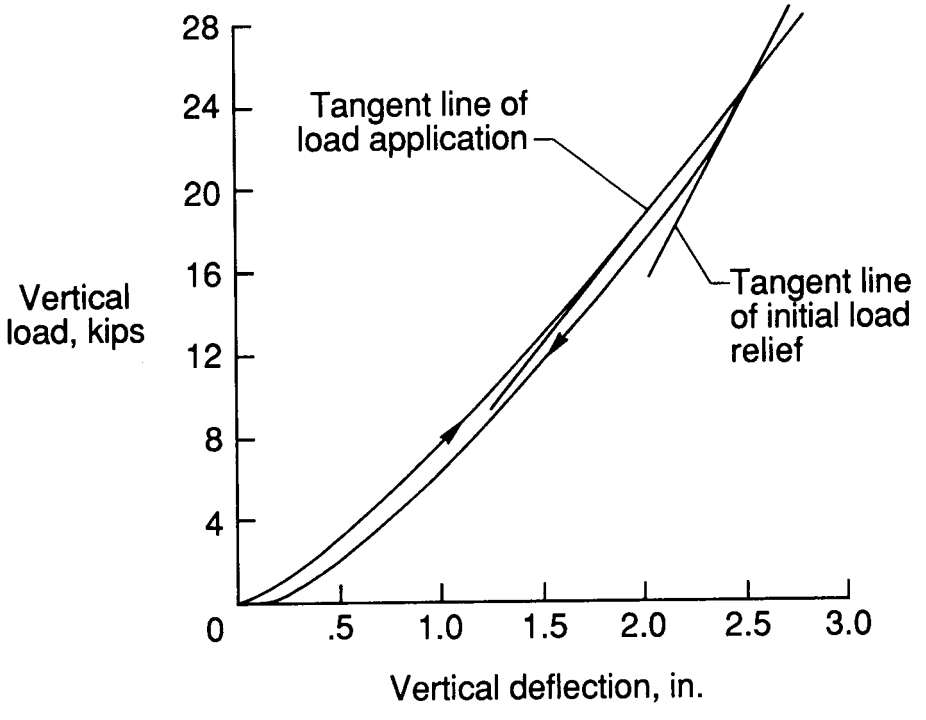

Figure 9. Vertical-load-deflection curve of radial-belted tire at inflation pressure of 310 psi.

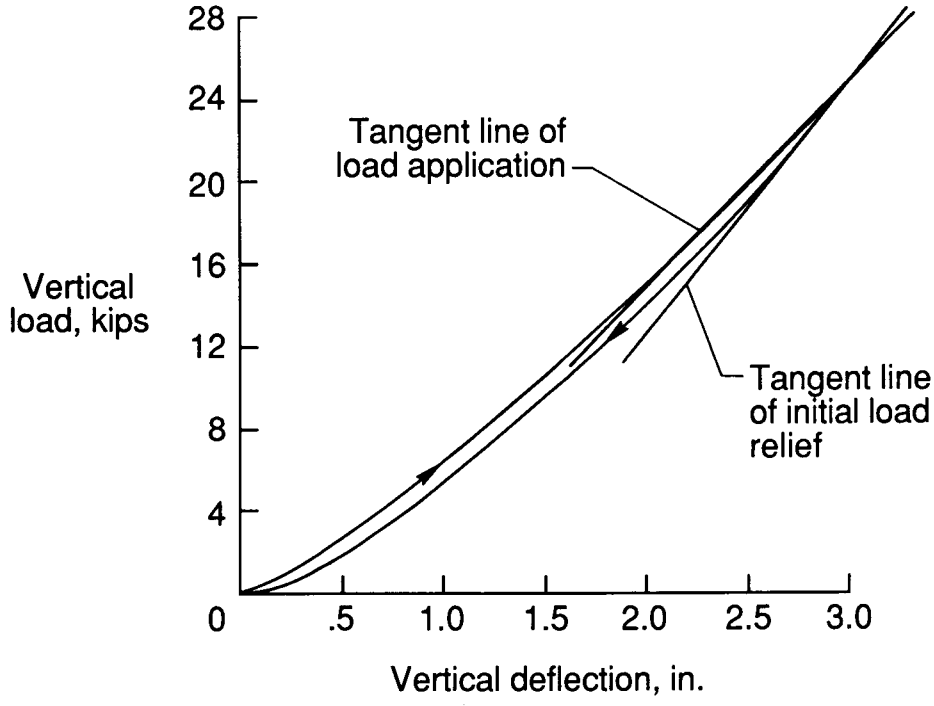

Figure 10. Vertical-load-deflection curve of radial-belted tire at inflation pressure of 245 psi.

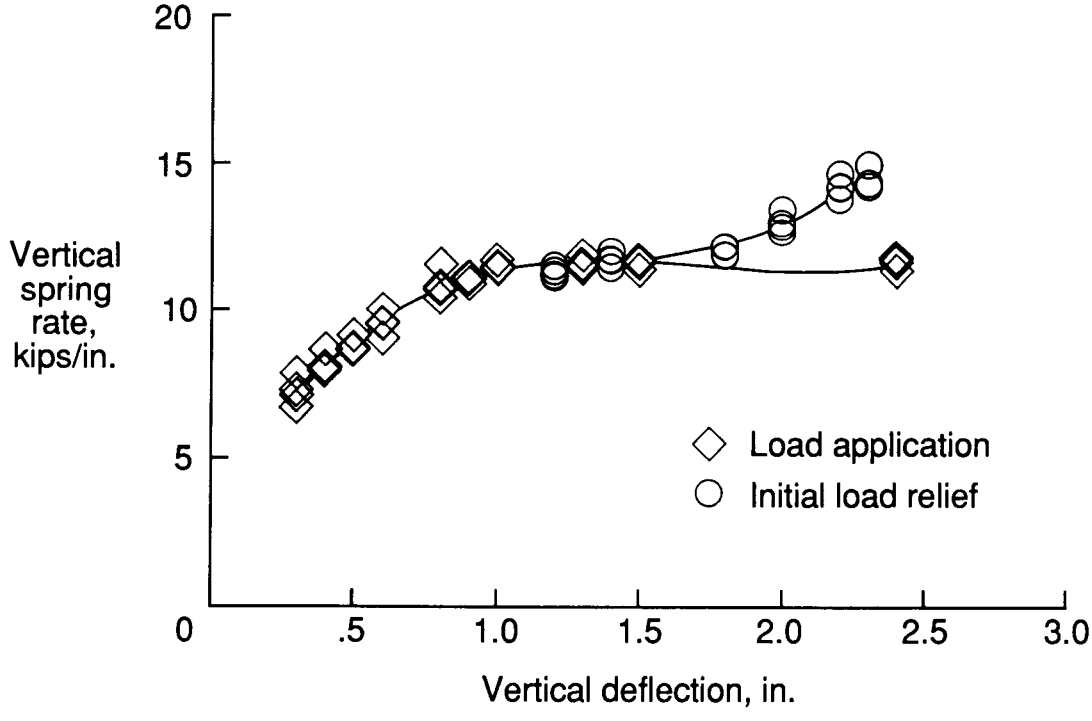

Figure 11. Vertical spring rate of bias-ply tire at inflation pressure of 245 psi.

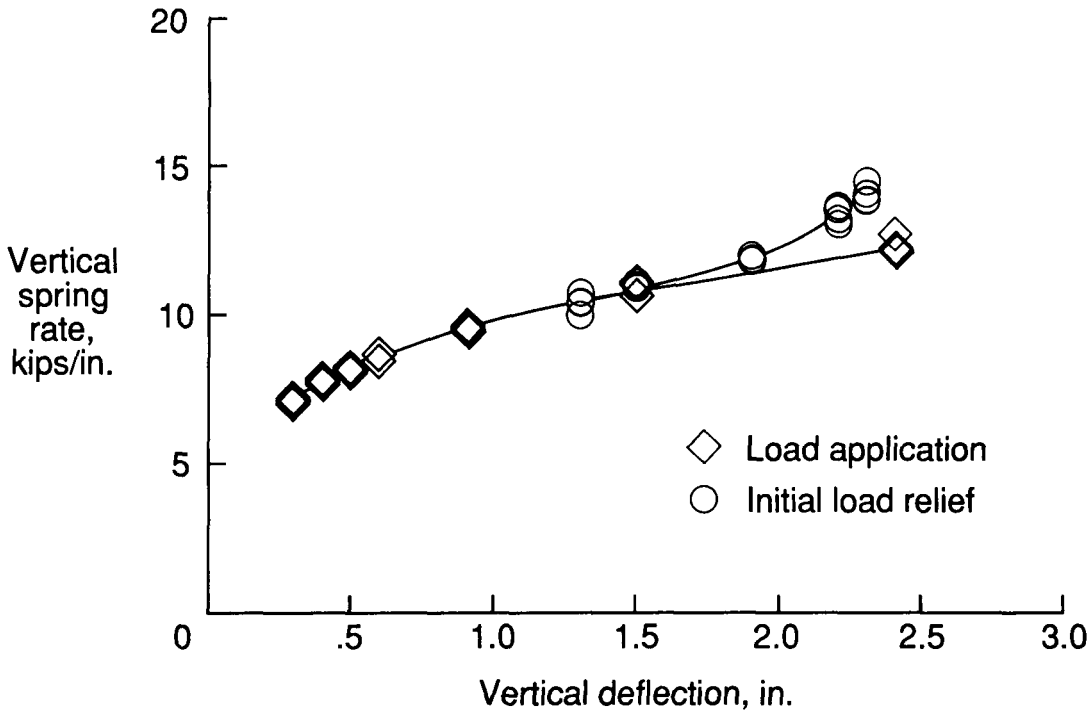

Figure 12. Vertical spring rate of radial-belted tire at inflation pressure of 310 psi.

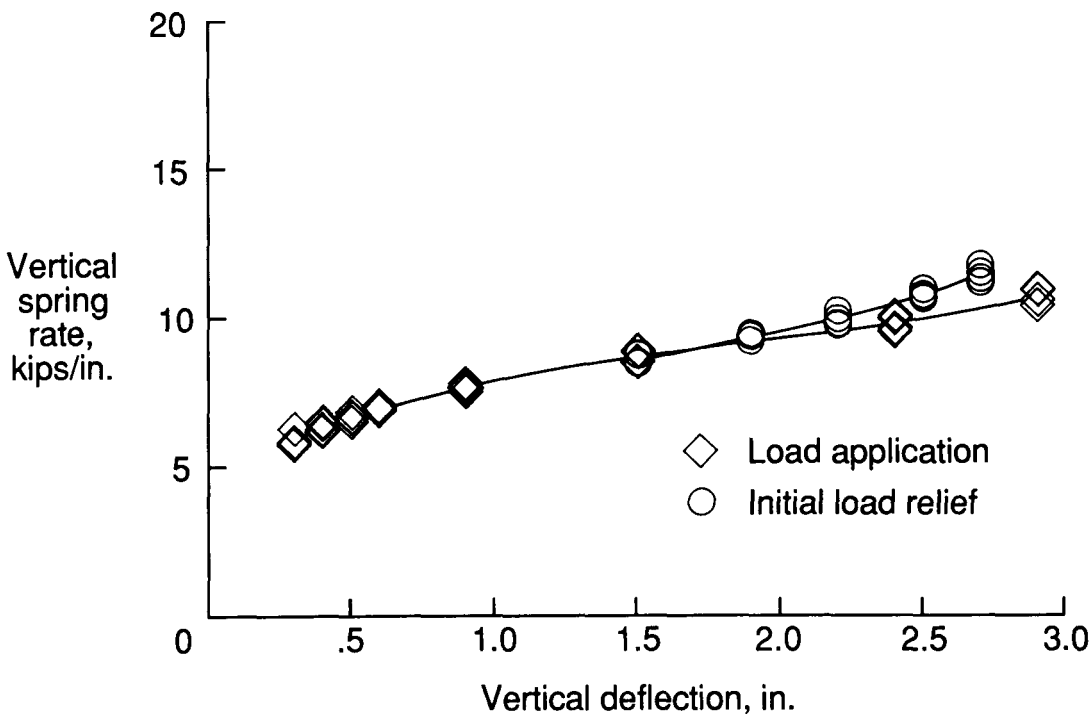

Figure 13. Vertical spring rate of radial-belted tire at inflation pressure of 245 psi.

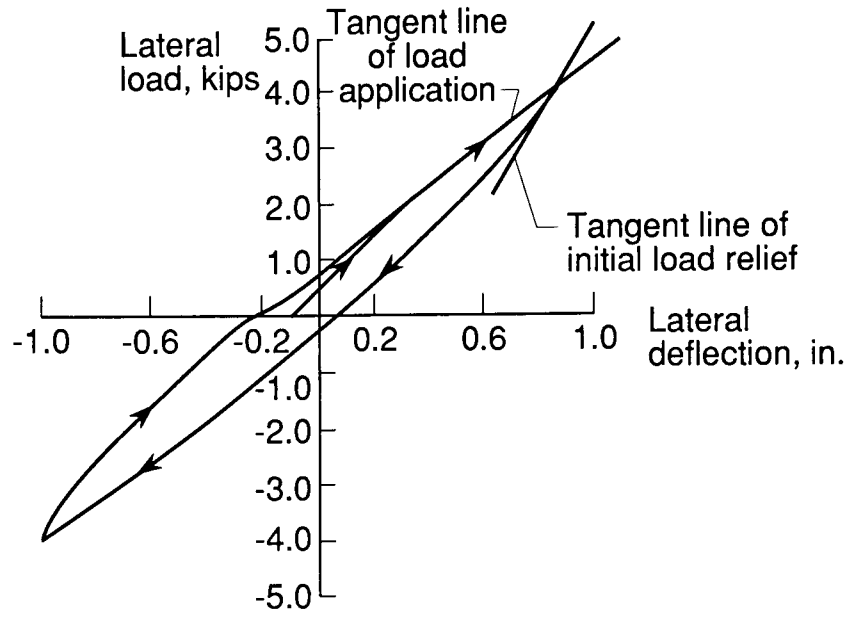

Figure 14. Lateral-load-deflection curve of bias-ply tire at inflation pressure of 245 psi.

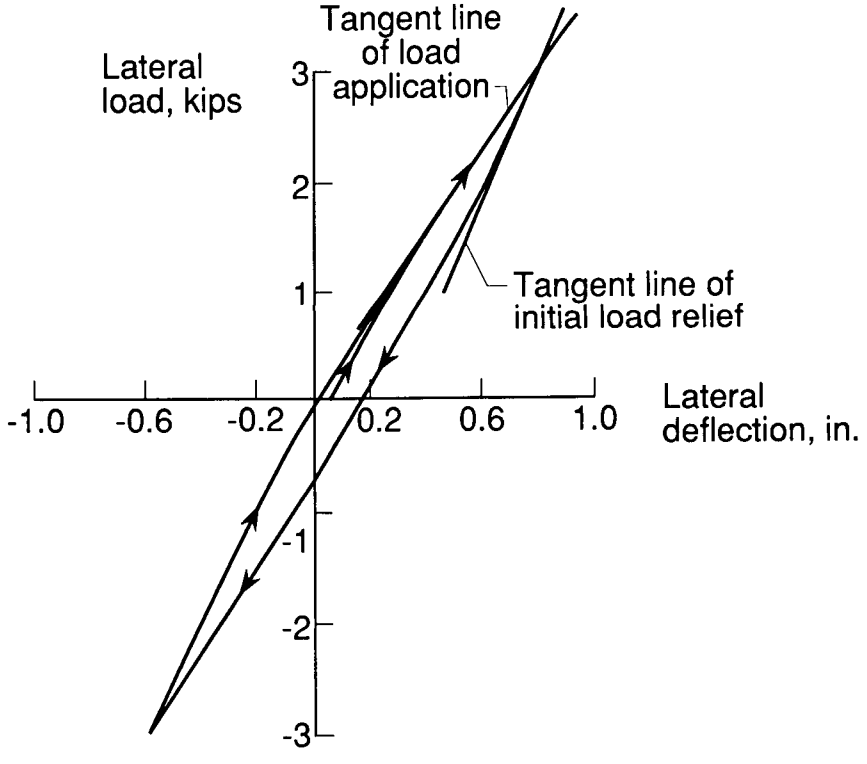

Figure 15. Lateral-load-deflection curve of radial-belted tire at inflation pressure of 310 psi.

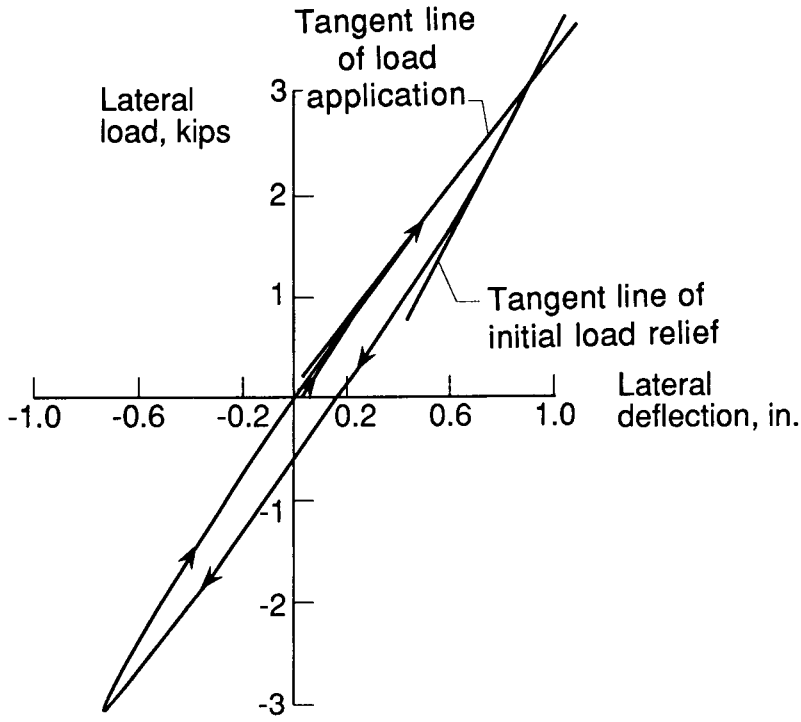

Figure 16. Lateral-load-deflection curve of radial-belted tire at inflation pressure of 245 psi.

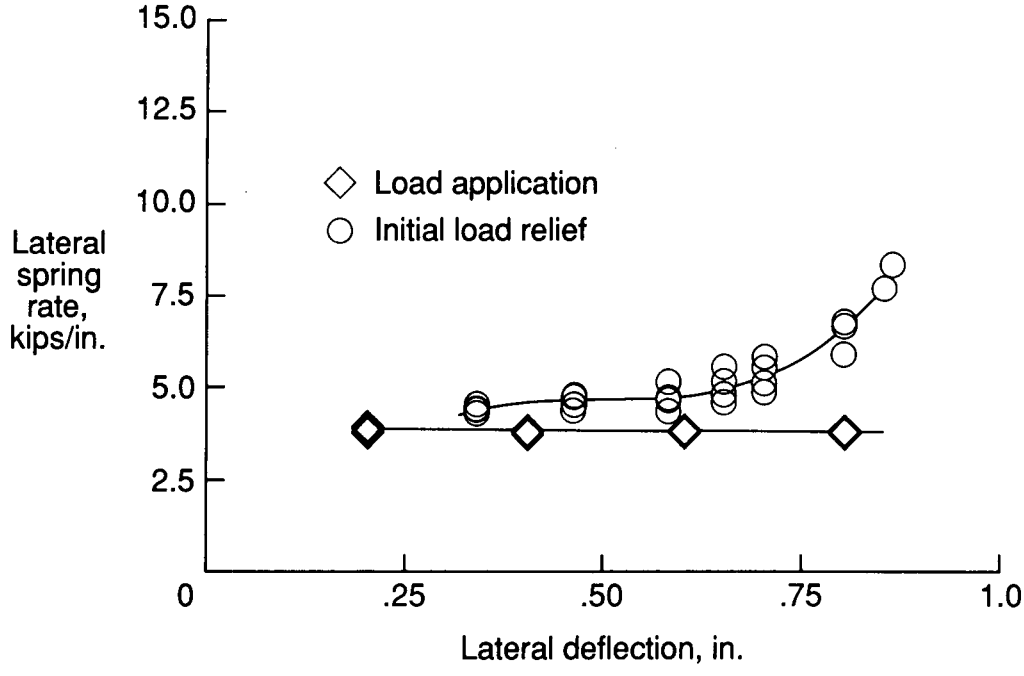

Figure 17. Lateral spring rate of bias-ply tire at inflation pressure of 245 psi.

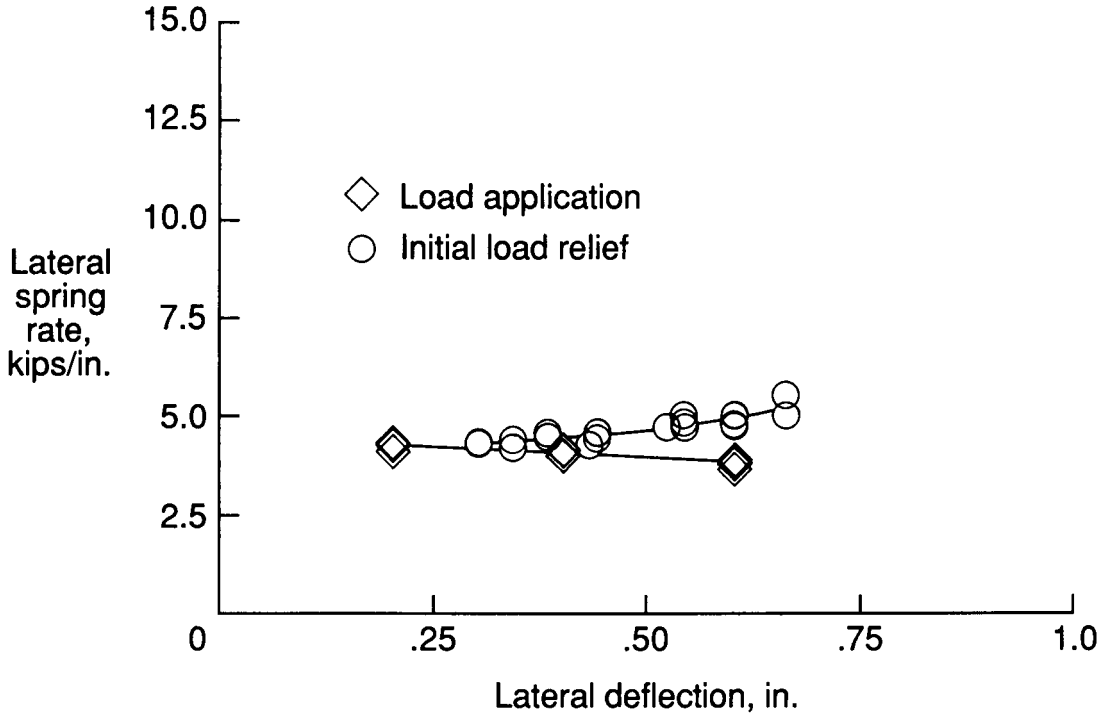

Figure 18. Lateral spring rate of radial-belted tire at inflation pressure of 310 psi.

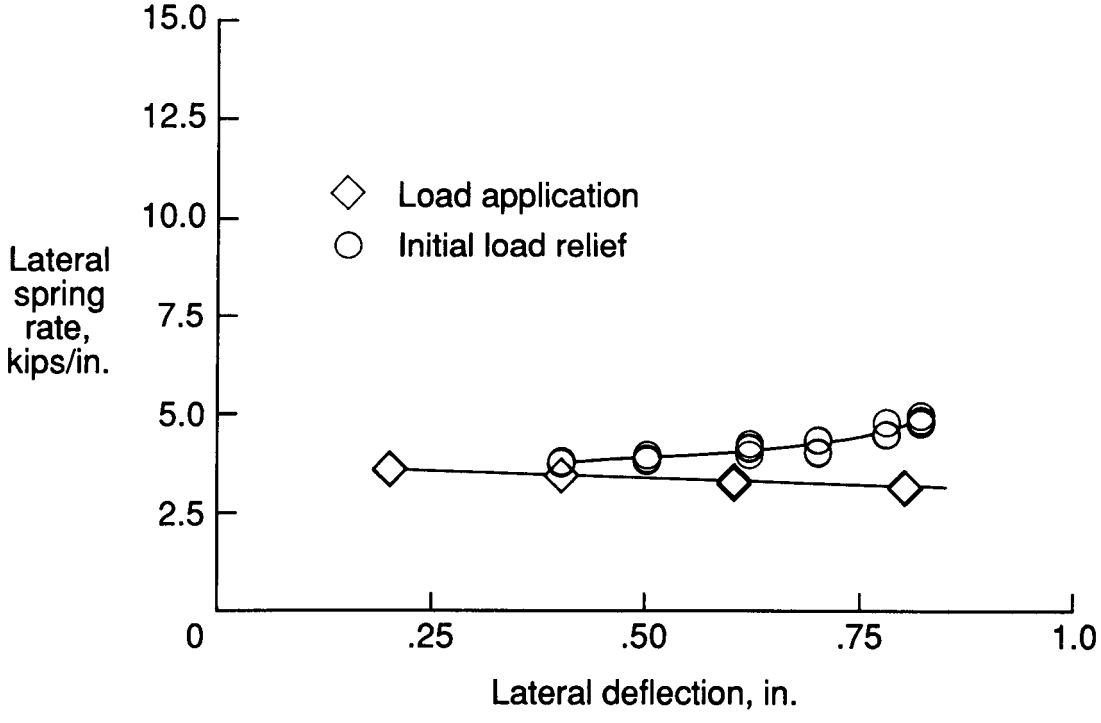

Figure 19. Lateral spring rate of radial-belted tire at inflation pressure of 245 psi.

NASA
National Aeronautics and Space Administration

Report Documentation Page

1. Report No.	2. Government Accession No.	3. Recipient's Catalog No.
NASA TP-2810		

4. Title and Subtitle	5. Report Date
Static Mechanical Properties of 30×11.5 – 14.5, Type VIII Aircraft Tires of Bias-Ply and Radial-Belted Design	May 1988
	6. Performing Organization Code
7. Author(s)	8. Performing Organization Report No.
Pamela A. Davis and Mercedes C. Lopez	L-16374
	10. Work Unit No.
9. Performing Organization Name and Address	505-63-41-02
NASA Langley Research Center Hampton, VA 23665-5225	11. Contract or Grant No.
	13. Type of Report and Period Covered
12. Sponsoring Agency Name and Address	Technical Paper
National Aeronautics and Space Administration Washington, DC 20546-0001	14. Sponsoring Agency Code

15. Supplementary Notes

16. Abstract

An investigation was conducted to determine the static mechanical properties of a 30 × 11.5 – 14.5, type VIII, bias-ply and radial-belted aircraft tire. The properties measured were the spring rate and damping characteristics of each tire from vertical- and lateral-loading hysteresis loops. Mass moment of inertia tests were also conducted. The results of the study are presented along with a discussion of the advantages and disadvantages of each type of tire.

17. Key Words (Suggested by Authors(s))

Radial-belted tire
Bias-ply tire
30 × 11.5 – 14.5, type VIII aircraft tire
Static mechanical properties

18. Distribution Statement

Unclassified—Unlimited

Subject Category 05

19. Security Classif.(of this report)	20. Security Classif.(of this page)	21. No. of Pages	22. Price
Unclassified	Unclassified	24	A02

NASA FORM 1626 OCT 86

NASA-Langley, 1988

For sale by the National Technical Information Service, Springfield, Virginia 22161-2171